

Fig. 7.1. Different interface inclinations

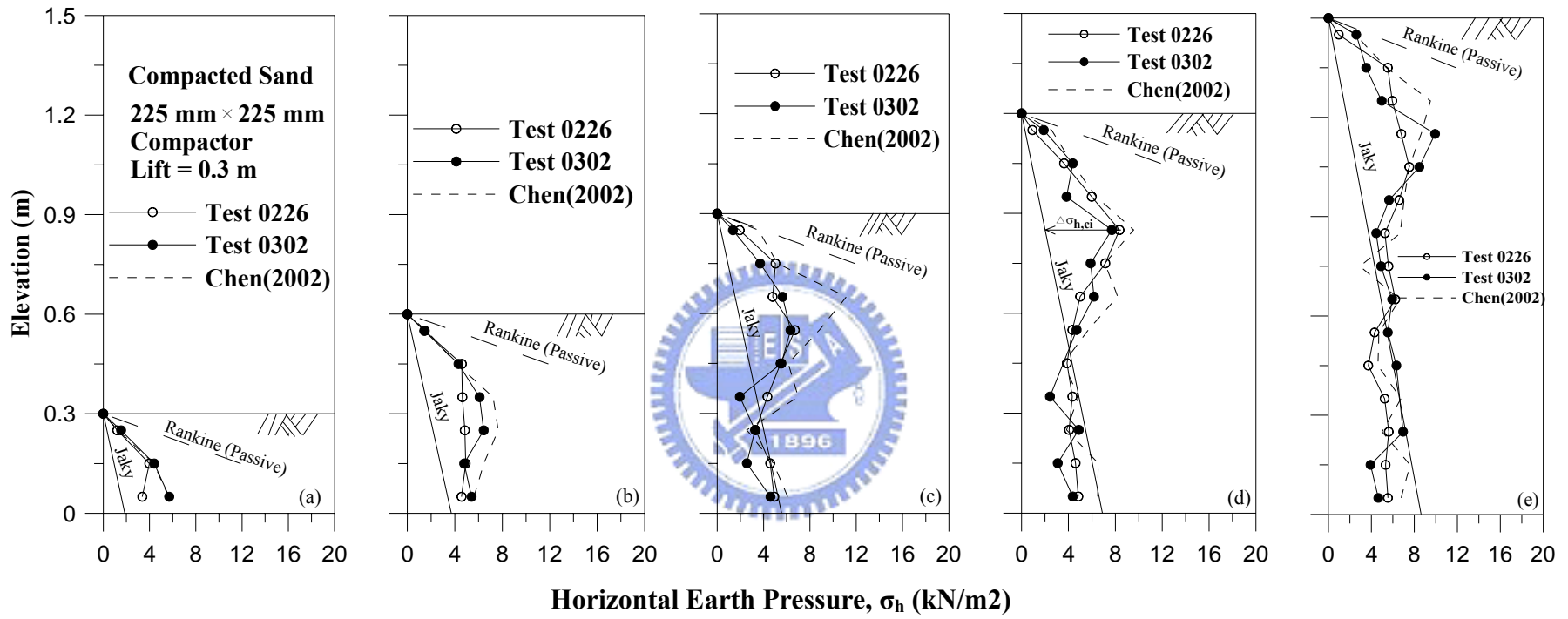


Fig. 7.2. Distribution of lateral earth pressure at $\alpha = 0^\circ$ for sand compacted with a square compactor

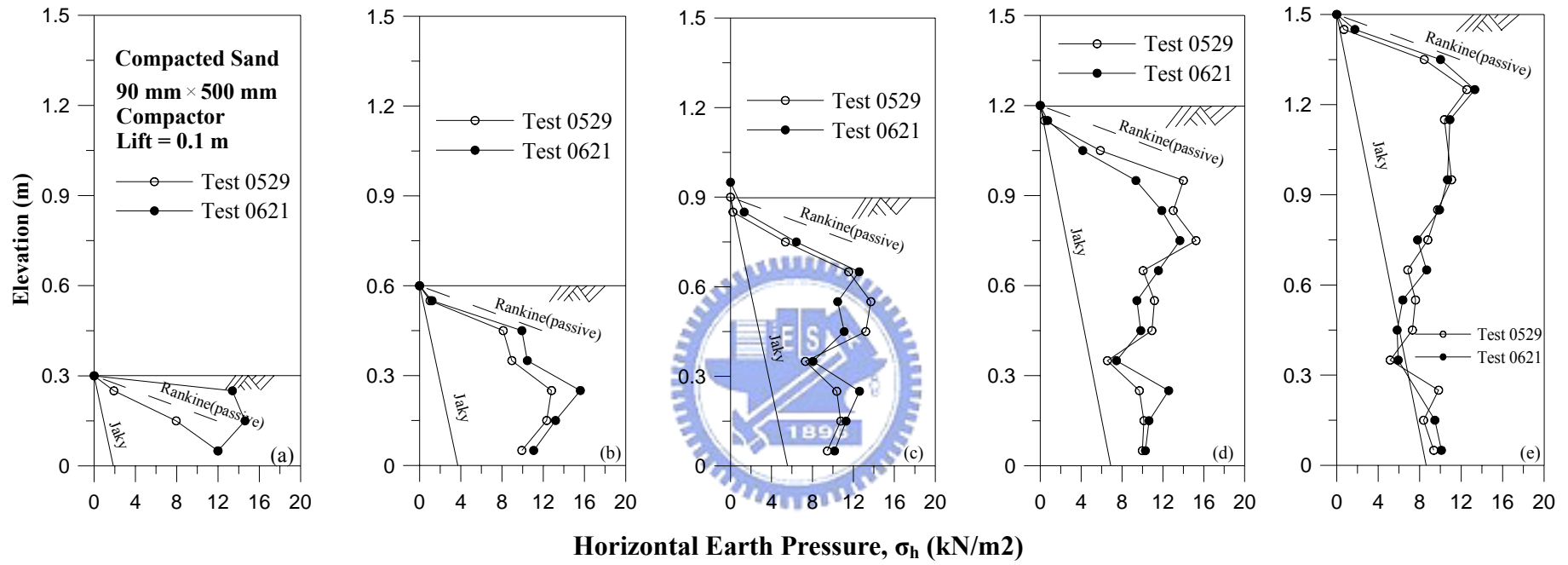


Fig. 7.3. Distribution of lateral earth pressure at $\alpha = 0^\circ$ for sand compacted with strip compactor

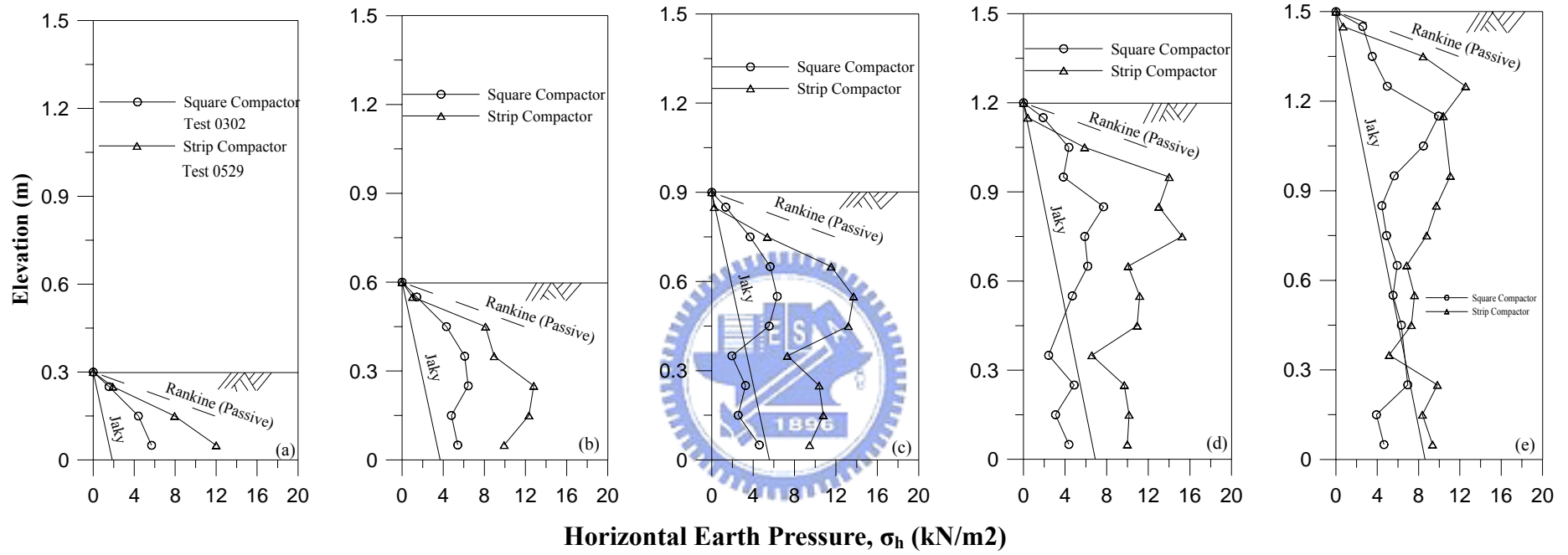
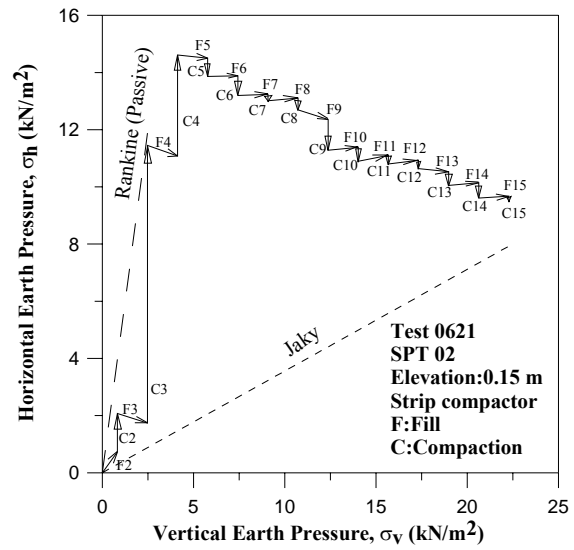
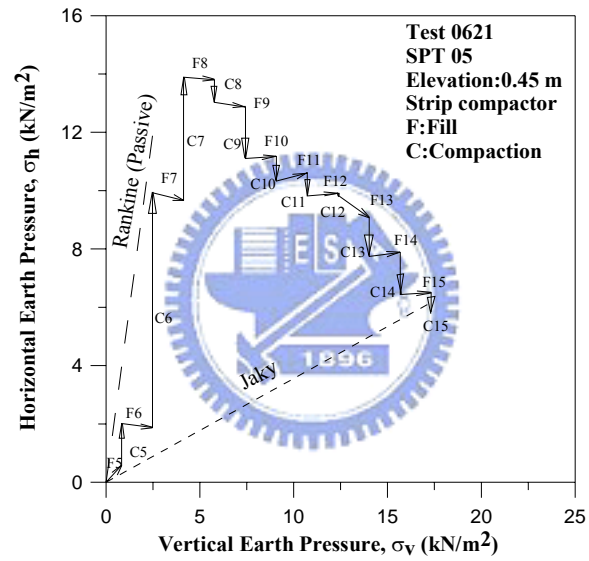


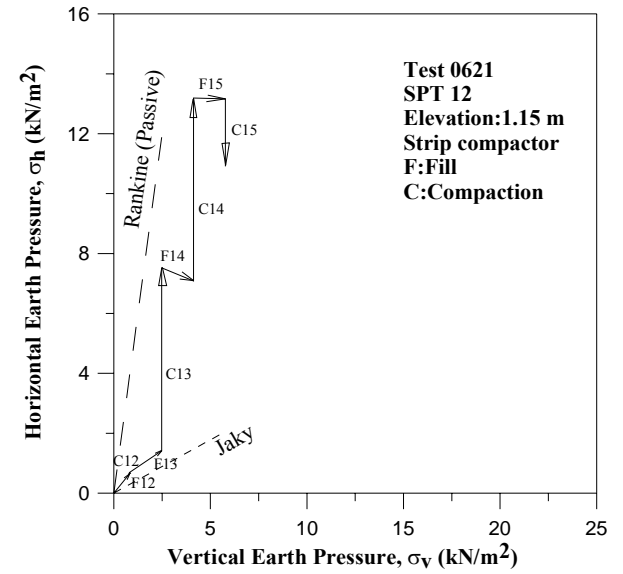
Fig. 7.4. Comparison of lateral earth pressure at $\alpha = 0^\circ$ for compacted sand



(a)

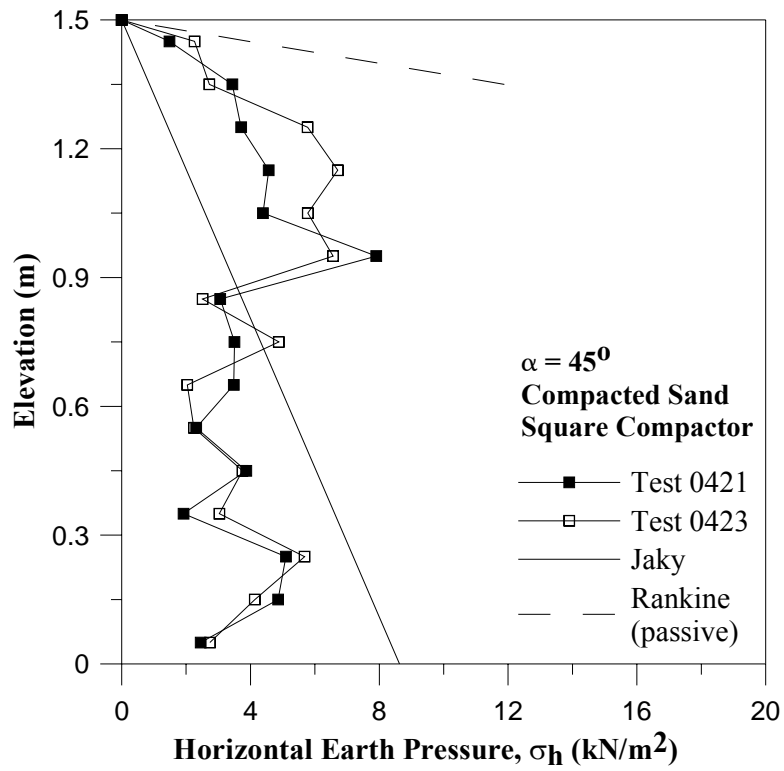


(b)

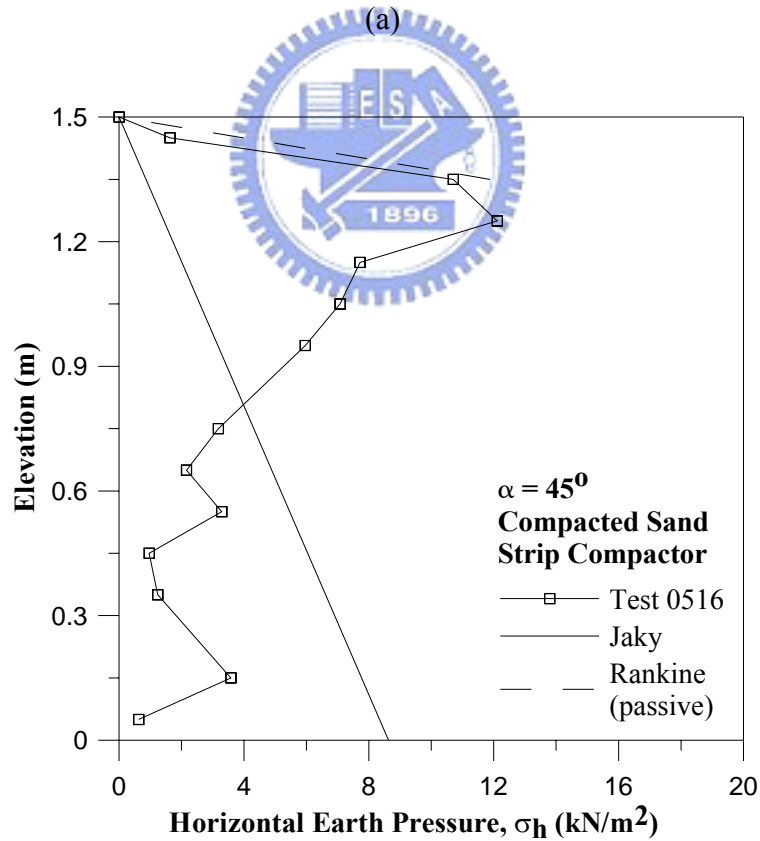


(c)

Fig. 7.5. Stress path of a soil element under compaction

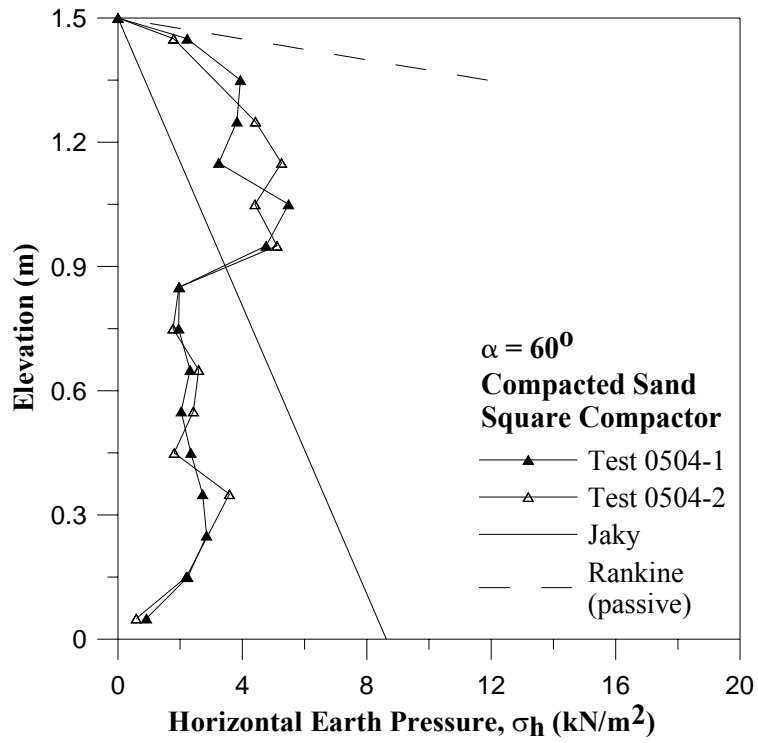


(a)

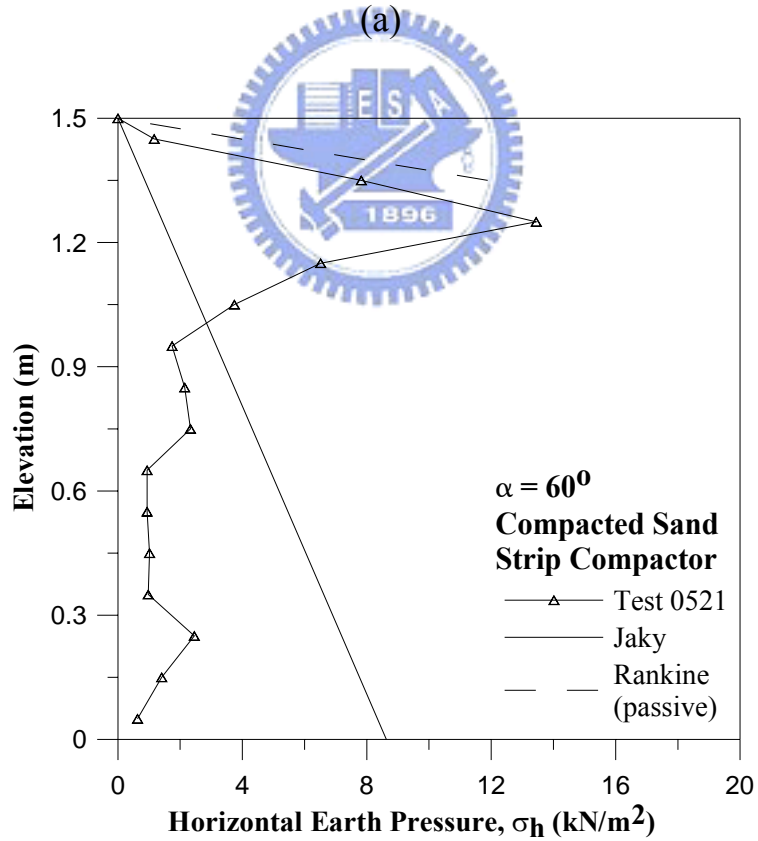


(b)

Fig. 7.6. Distribution of lateral earth pressure at $\alpha = 45^\circ$ for compacted sand



(a)



(b)

Fig. 7.7. Distribution of lateral earth pressure at $\alpha = 60^\circ$ for compacted sand

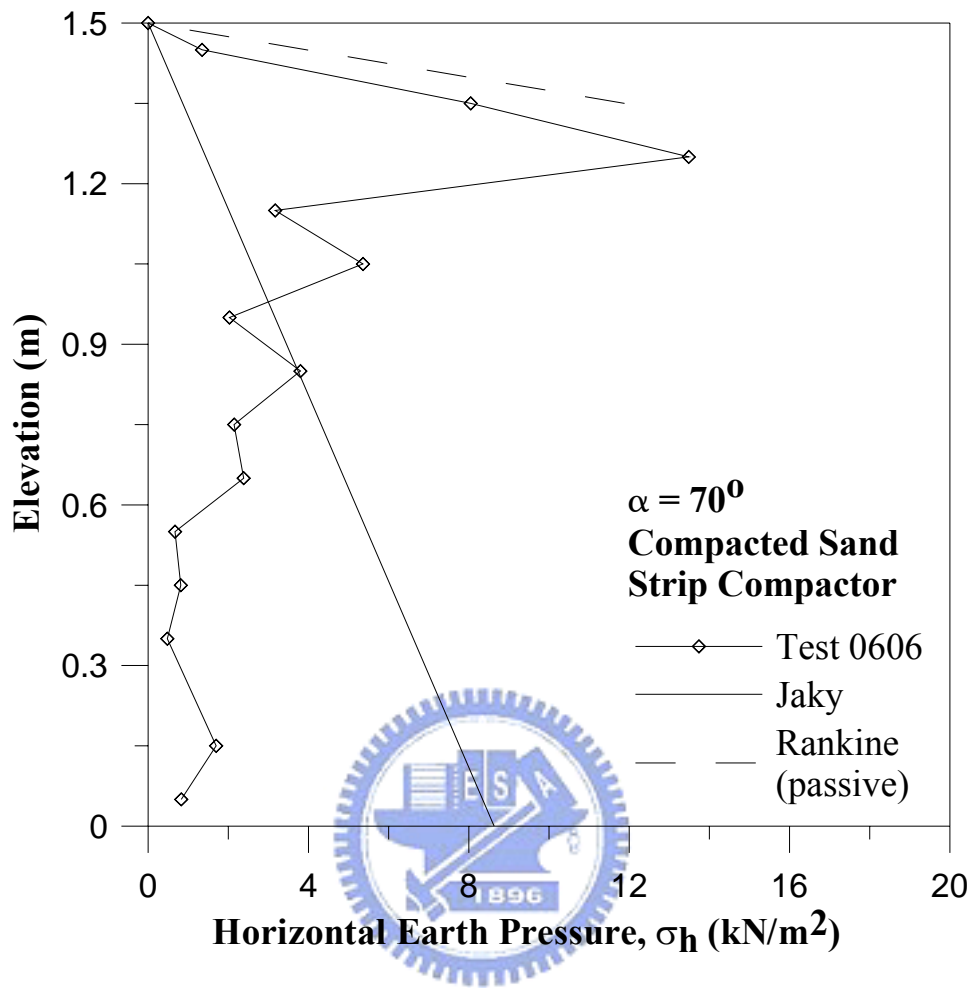


Fig. 7.8. Distribution of lateral earth pressure at $\alpha = 70^\circ$ for compacted sand

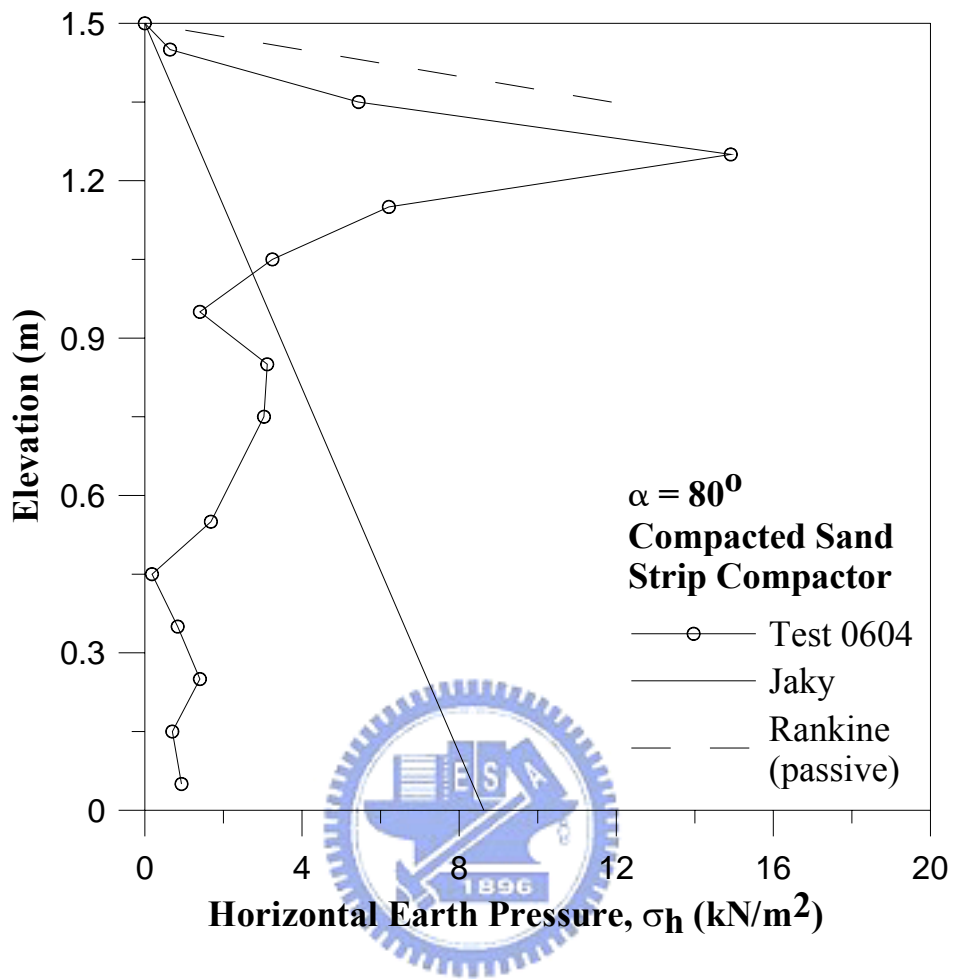


Fig. 7.9. Distribution of lateral earth pressure at $\alpha = 80^\circ$ for compacted sand

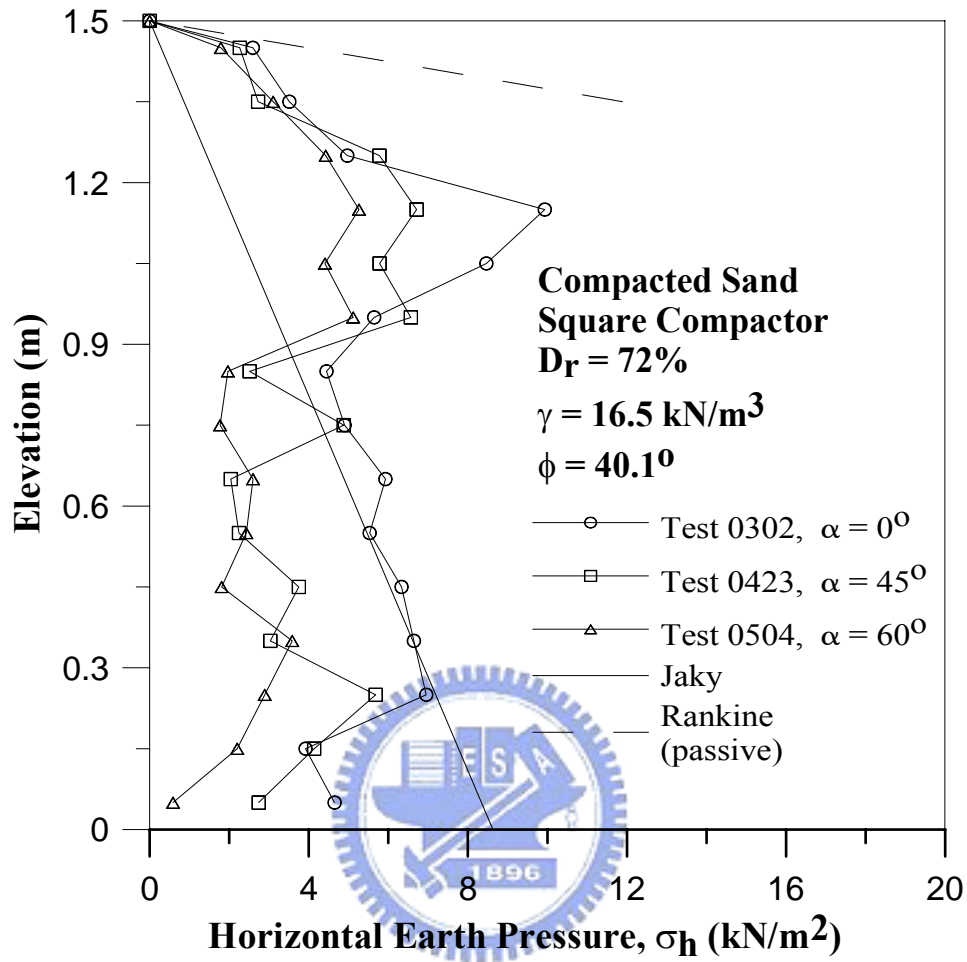


Fig. 7.10. Distribution of lateral earth pressure at various α for sand compacted with square compactor

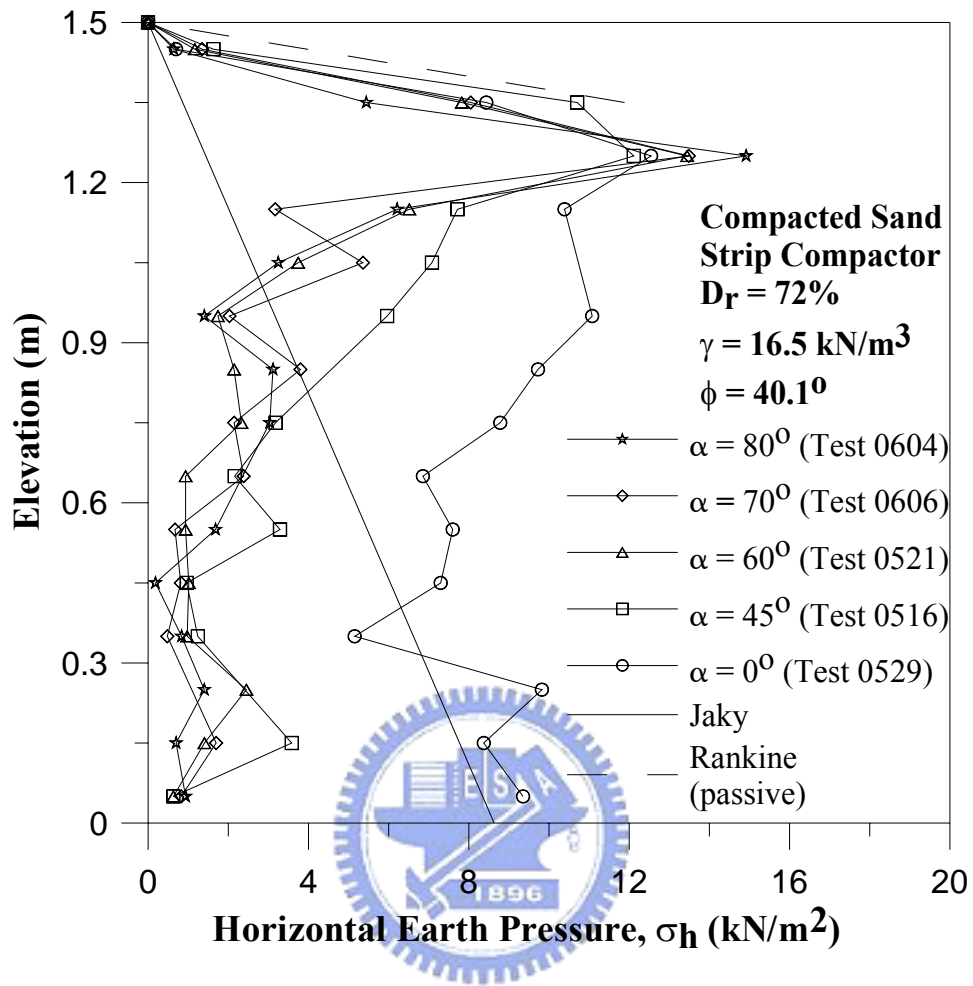


Fig. 7.11. Distribution of lateral earth pressure at various α for sand compacted with strip compactor

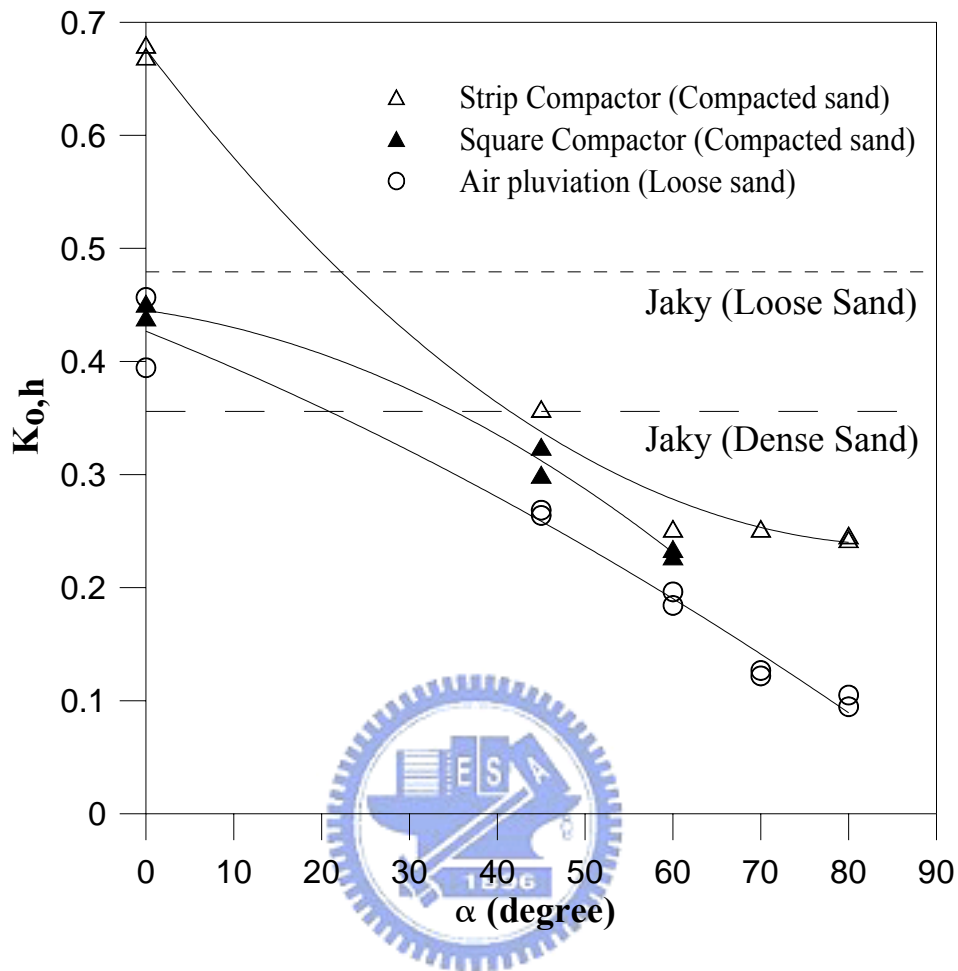
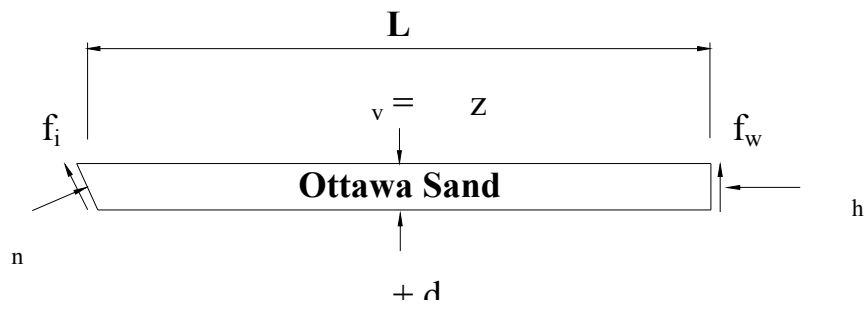
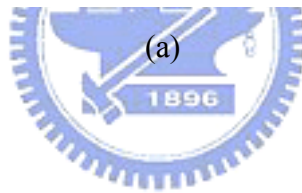
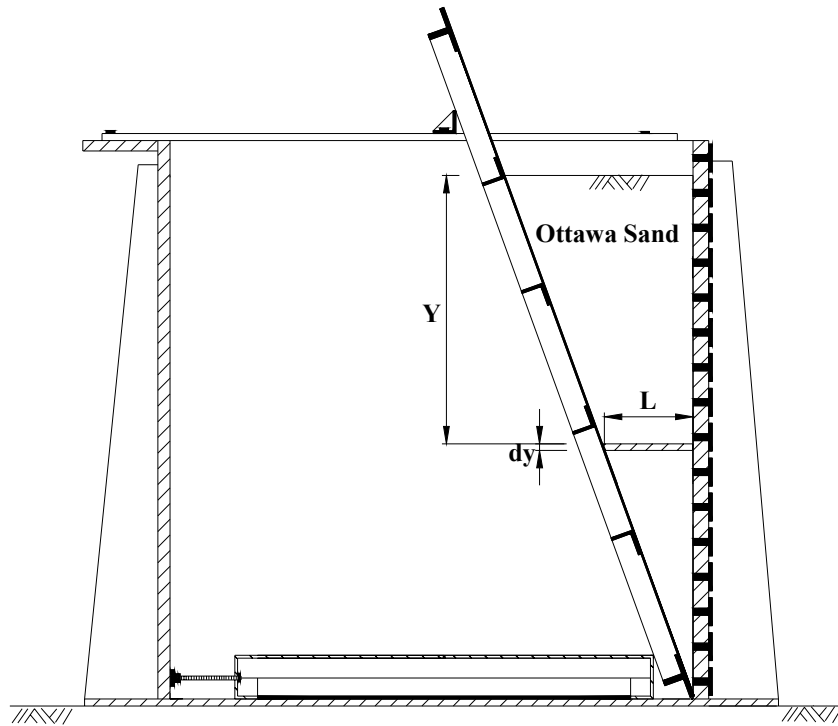


Fig. 7.12 Variation of $K_{o,h}$ at various α



(b)

Fig. 7.13 Horizontal lamina of Ottawa sand

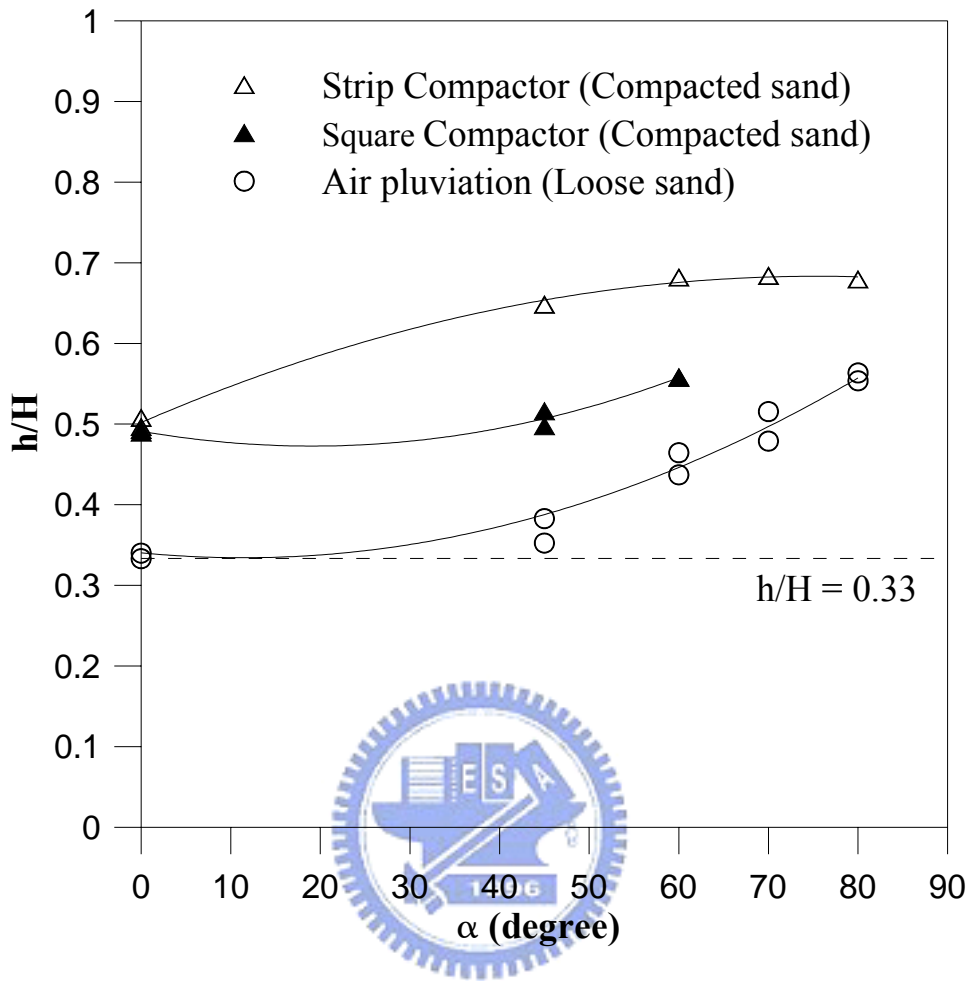


Fig. 7.14. Point of application of resultant force at various α

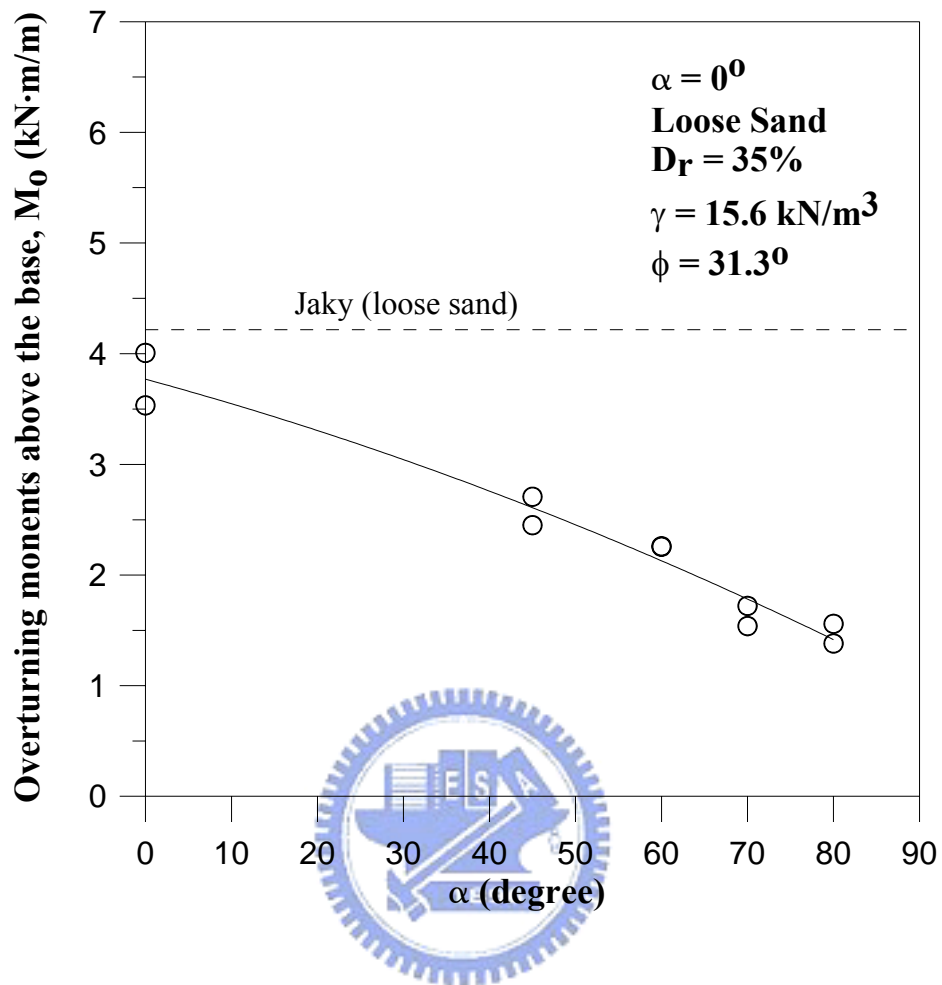


Fig. 7.15. Overturning moments about the base, M_o at various